

Aggregation behavior of the surfactant bearing pyrrolidinium head group in the presence of polyacrylic acid*

E. A. Vasilieva,* S. S. Lukashenko, L. A. Vasileva, R. V. Pavlov, G. A. Gaynanova, and L. Ya. Zakharova

A. E. Arbuzov Institute of Organic and Physical Chemistry, Federal Research Center
"Kazan Scientific Center of the Russian Academy of Sciences,"
8 ul. Akad. Arbuzova, 420088 Kazan, Russian Federation.
Fax: +7 (843) 273 1872. E-mail: vasilevaelmira@mail.ru

The aggregation characteristics of binary systems based on a novel pyrrolidinium surfactant with the hexadecyl hydrocarbon tail and hydroxyethyl fragment at the nitrogen atom were studied in the presence of polyacrylic acid by a complex of physicochemical methods (tensiometry, conductometry, dynamic light scattering, fluorescence spectroscopy, and spectrophotometry). The formation of surfactant–polyelectrolyte complexes leads to a decrease in the concentration thresholds of aggregation by an order of magnitude to form aggregates ~70 nm in size was established by tensiometry and fluorimetry. The solubilization capacity of the formed mixed aggregates was tested using the Orange OT hydrophobic dye.

Key words: pyrrolidinium surfactant, polyacrylic acid, polyelectrolyte–surfactant complex, critical aggregation concentration.

Cationic amphiphiles capable of forming supramolecular structures of various morphology (direct and reverse micelles, vesicles, liquid crystals, *etc.*) in solutions remain to be the subject of basic and applied research for a long time.^{1–4} Therefore, the target synthesis of surfactants (Surf) is one of the promising trends in the development of this area.⁵ Surfactants with the cyclic head group, including those based on pyrrolidine derivatives (PS), differed in geometry from classic surfactants of the trimethylammonium series attract special attention. The micelle forming ability and surface activity of PS are higher than those of alkyltrimethylammonium bromides. In addition, their morphological behavior is much more complicated. The aggregation properties of *N*-alkyl-*N*-methylpyrrolidinium bromides with the variation of the nature of counterion, solvent, alkyl radical length, *etc.* are described.^{6–11} The thermodynamic parameters of the micelle formation of PS in water,⁵ ethylammonium nitrate,¹¹ and in mixtures¹² were studied. The system based on geminal surfactants with the pyrrolidinium head group were also studied.¹³

At the same time, we showed^{14,15} that the introduction of the hydroxyalkyl group into the structures of cationic surfactants can substantially decrease the critical micelle concentration (CMC) values due to the formation of additional hydrogen bonds. Therefore, we have earlier synthesized a series of cationic surfactants with the pyr-

rolidinium head group bearing the hydroxyethyl fragment at the nitrogen atom. Their aggregation properties and antimicrobial activity were characterized.¹⁶ It is shown that the introduction of the hydroxyethyl fragment into the composition of the head group results in a twofold increase in the micelle forming ability of these amphiphiles compared to the unsubstituted analogs. The CMC values of the pyrrolidinium surfactants are lower than the CMC of the closest analogs with the heterocyclic head group (alkylimidazolium¹⁷ and alkylmorpholinium¹⁸ bromides) at the same hydrophobicity.

There are single works devoted to the study of binary systems based on PS in the presence of other amphiphiles or polymers.^{19,20} For example, the formation of ion pairs between PS bearing the dodecyl radicals and sodium dodecyl sulfate resulting in the formation of vesicles on reaching the concentration threshold of aggregation was shown.¹⁹ Vesicles are also formed in a PS–Pluronic F108 system, and higher degrees of loading and solubilization of quercetin compared to the individual aggregates are observed.²⁰ It is known that the formation of complexes between surfactants and polymers (polyelectrolytes) when the critical aggregation concentration (CAC) is achieved can result in a change in the functional properties of individual components to a significant extent.²¹

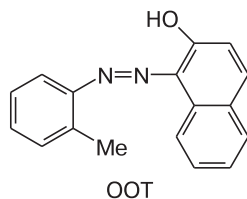
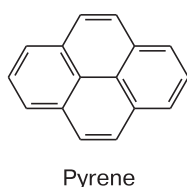
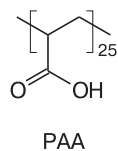
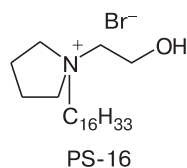
This work is aimed at determining regularities of the self-organization in aqueous solutions of the novel cationic amphiphile with the pyrrolidinium head group containing the hydroxyethyl fragment and hexadecyl hydrocarbon radical in the presence of polyacrylic acid. The interaction

* Dedicated to Academician of the Russian Academy of Sciences A. I. Konovalov on the occasion of his 85th birthday.

in the systems based on the cationic surfactant and polyelectrolyte (PE) was comprehensively evaluated, which is interesting from both the fundamental (modeling of processes occurring in living organisms) and practical (compositions of cosmetic products, detergents, food substances, *etc.*) points of view.

Experimental

Polyacrylic acid (PAA, $M_r = 1800 \text{ g mol}^{-1}$), pyrene, Orange OT (OOT) were commercially available from Sigma-Aldrich and used as received. *N*-(2-Hydroxyethyl)-*N*-hexadecylpyrrolidinium bromide (PS-16) was synthesized by our previously described procedure.¹⁶ Solutions were prepared using water purified with a Direct-Q5 system (Millipore, France), and its specific resistance was 18.2 MOhm cm. Samples of the studied systems were examined at 25 °C in temperature-maintained cells.



Tensiometry. The ring detachment method was applied to determine the surface tension of the studied solutions on a K6 tensiometer (Kruss, Germany) using a platinum–iridium ring 20 mm in diameter hanged to a precise balance. The measurements were performed until a stable value was obtained (at least five times). The measurement error did not exceed 3%.

Conductometry. The conductivity (χ) was measured on an InoLab Cond 7110 conductometer (WTW, Germany) with a TetraCon remote sensor.

Spectrophotometry. The solubilization capacity of surfactant aggregates was determined using the OOT spectral probing dye. To obtain a saturated solution, the dye (0.0014 g) was added to a solution of the surfactant (2 mL), the mixture was stirred and kept for 48 h, the solution was filtered, and the absorbance was measured at 495 nm. Absorption spectra were recorded on a Specord 250 Plus spectrophotometer (Analytik Jena, Germany). Glass cells 1 and 0.5 cm thick were used for measurements.

Fluorimetry. Pyrene was used as a fluorescent probe to determine the CAC of solutions by the fluorimetric method on a Varian Cary Eclipse spectrofluorimeter (Agilent, USA) in quartz cells 1 cm thick. The initial solution of pyrene in ethanol was added to the studied Surf–PE solutions in such a way that the fluorophore concentration in the solution would be $1 \cdot 10^{-6} \text{ mol L}^{-1}$. The excitation wavelength for pyrene was 335 nm, and the emission spectra were recorded in the range from 350 to 500 nm.

Turbidimetry. The phase behavior of Surf–PAA mixed systems was studied on a Specord 250 Plus spectrophotometer (Germany). A fixed volume of a PAA solution was added to solutions

of the surfactant, the mixture was kept for 2 min, and the absorbance of the solutions was measured at a wavelength of 500 nm.

Dynamic and electrophoretic light scattering. Experiments on dynamic light scattering were carried out on a Zetasizer Nano ZS instrument (Malvern, Great Britain) to determine the size and ζ -potential of the obtained aggregates in the studied solutions. A He–Ne gas laser served as a radiation source. The laser power was 10 mW, the wavelength was 633 nm, and the light scattering angle was 173°. The effective hydrodynamic diameter was calculated automatically from the diffusion coefficients using the Stokes–Einstein equation for spherical particles

$$D = k_B T / (6\pi\eta R_h),$$

where k_B is the Boltzmann constant, T is absolute temperature, and η is the solvent viscosity.

Measurements were conducted at least five times to obtain the average value.

Potentiometry. The pH of the medium was determined on a pH-211 instrument (Hanna Instruments, Germany). The temperature of the solutions was maintained at 25 °C with a thermostat. The measurement accuracy was 0.05 pH units. The glass electrode was calibrated by standard solutions.

Results and Discussion

The binary systems were studied at a variable surfactant concentration and the fixed PAA concentration (1, 3, and 5 mmol L⁻¹). The dissolution of PAA in water gives a solution with pH 4, which corresponds to the degree of ionization ~8%, *i.e.*, under these conditions, PE weakly dissociates in individual and mixed systems. Since the PE–Surf mixed system consists of oppositely charged components, the formation of stoichiometric complex can be accompanied by the appearance of turbidity or precipitation. Therefore, the phase behavior of the PAA–PS-16 mixed system was studied before investigation of its aggregating ability.

The turbidimetry data presented in Fig. 1 demonstrate the change in the phase state with an increase in the surfactant concentration in the PAA–PS-16 binary system. An unusual situation is observed: at low surfactant concentrations the solutions are slightly turbid regardless of the PAA concentration. This indicates that the surfactant begins to compensate the charge of the polyacid even at low concentrations. Probably, the effective charge compensation is related to an insufficiently large head group of the amphiphile. The turbidity indicates the formation of a stoichiometric complex when the system loses the charge. As known, the charge stabilizes colloidal system and prevents particle adhesion. A small region is observed with the further increase in the surfactant concentration where the solutions remain transparent. However, when a certain surfactant concentration is achieved, the solutions become turbid and reach the maximum absorbance, but no phase separation occurs. The absorbance decreases with the further increase in the surfactant concentration, and the solutions gradually become transparent again.

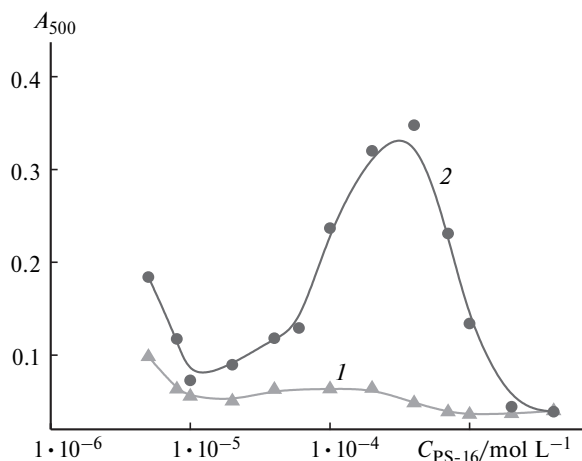


Fig. 1. Absorbance at 500 nm (A_{500}) of a PAA–PS-16 binary system vs PS-16 concentration at the PAA concentrations 1 (1) and 3 mmol L⁻¹ (2) (pH 4, $t = 25$ °C).

The Surf–PE interaction induces association at the very low surfactant concentration (CAC), which is lower, as a rule, than the CMC of an individual solution of the surfactant. At the first stage of the work, the CAC values of the mixed systems were determined by tensiometry. The dependences of the surface tension of PAA–PS-16 binary systems on the surfactant concentration are presented in Fig. 2. Two inflections are observed on the concentration curves of the PAA–PS-16 mixed systems. The first inflection shows the CAC₁ values, *i.e.*, the concentration at which mixed aggregates begin to form. The second inflection corresponds to the CAC₂, *i.e.*, the concentration corresponding to the formation of free surfactant aggregates after the polymer chain is saturated by the surfactant aggregates. The second break in the concentration curve of the surface tension becomes more pronounced with an increase in the PAA concentration. The highest synergic effect of the interaction of the components is observed for the minimum concentration of PAA (1 mmol L⁻¹): the CAC₁ values of the PAA–PS-16 system by tensiometry (0.02 mmol L⁻¹) are an order of magnitude lower than the CMC of an individual micellar solution of PS-16 (0.42 mmol L⁻¹). Higher PE concentrations slightly shift

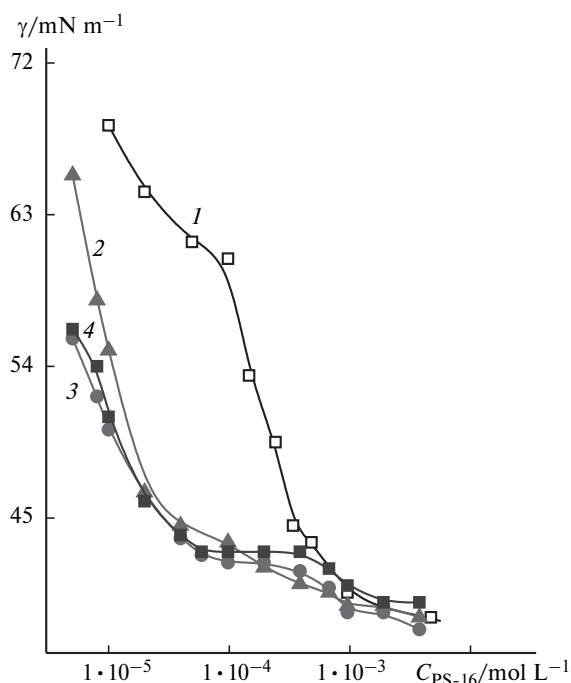


Fig. 2. Surface tension isotherms in an individual solution of PS-16 (1) and in PAA–PS-16 binary systems at the PAA concentrations 1 (2), 3 (3), and 5 mmol L⁻¹ (4) (pH 4, $t = 25$ °C).

the CAC of the mixed system to higher surfactant concentrations (0.035 mmol L⁻¹). A decrease in the CAC over the CMC is attributed to a decrease in the electrostatic repulsion of the head groups of the surfactant upon the addition of PE. The obtained CAC values are presented in Table 1.

The characteristics of the surface layer of PAA–PS-16 mixed solutions were calculated from the surface tension isotherms. As can be seen from Table 2, an additive of PAA to a solution of PS-16 leads to an increase in the minimum surface area per surfactant molecule (A_{\min}), and this parameter increases strongly with an increase in the PE concentration and the surface excess (Γ_{\max}) value, correspondingly, decreases. This probably means that a macromolecule loosens the dense packing of surfactant molecules at the interface. In the case of mixed systems, the free

Table 1. Values of CAC₁/CAC₂ and CAC (mmol L⁻¹) determined by different methods for PAA–PS-16 mixed systems

$C_{\text{PAA}}/\text{mmol L}^{-1}$	CAC ₁ /CAC ₂		CAC	
	Tensiometry	Spectrophotometry	Conductometry	Fluorimetry
0	0.42*	0.44*	0.36*	0.43*
1	0.02/0.85	0.1/0.94	0.74	0.04
3	0.035/1	0.27	0.9	0.05
5	0.031/1.3	0.43	1	0.03

* The CMC of an individual micellar solution of PS-16 is presented.

Table 2. Surface excess (Γ_{\max}), minimum surface area per surfactant molecule (A_{\min}), and standard free energies of adsorption (ΔG_{ad}) and micelle formation (ΔG_{m}) for PAA–PS-16 mixed systems (in the range of CAC)

C_{PAA} /mmol L ⁻¹	A_{\min} /nm ²	$\Gamma_{\max} \cdot 10^6$ /mol m ⁻²	$-\Delta G_{\text{m}}$	$-\Delta G_{\text{ad}}$
			kJ mol ⁻¹	
0	1.03	1.62	35.6	51.3
1	1.28	1.30	45.4	65.0
3	1.63	1.02	47.5	73.7
5	1.83	0.91	51.4	75.0

energies of micelle formation ΔG_{m} and adsorption ΔG_{ad} take more negative values than those for an individual solution of PS-16. This implies that the aggregation and adsorption of PS-16 in the presence of PAA are thermodynamically more favorable.

The breaks in the concentration curves of the electric conductivity make it possible to detect the thresholds of formation of combined Surf–PE aggregates. The dependences of the electric conductivity of PAA–PS-16 binary systems on the surfactant concentration are presented in Fig. 3. The curves have only one break, which is in good accordance with the CAC_2 value determined by tensiometry (see Table 1).

The data for PAA–PS-16 binary systems at different PAA concentrations obtained by fluorescence spectroscopy using pyrene as a hydrophobic probe are presented in Fig. 4. As can be seen from the plot, a polyelectrolyte addition to a solution of PS-16 leads to a decrease in the CMC value by one order of magnitude (from 0.43 to 0.04 mmol L⁻¹). An increase in the PAA concentration insignificantly affects the CAC. The data obtained are well consistent with the CAC values determined by tensio-

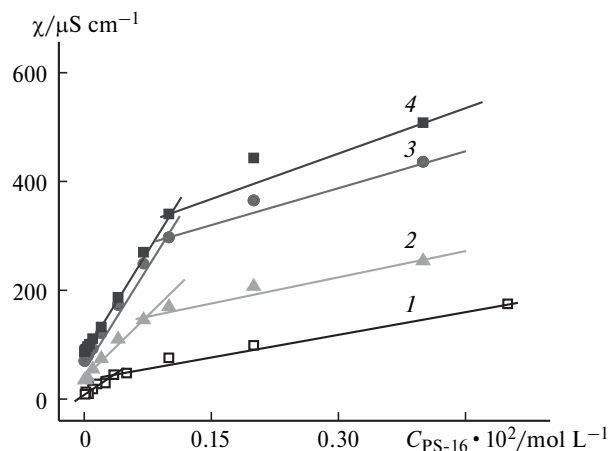


Fig. 3. Electric conductivity vs surfactant concentration in an individual solution of PS-16 (1) and in a PAA–PS-16 mixed system at the PAA concentration 1 (2), 3 (3), and 5 mmol L⁻¹ (4) (pH 4, $t = 25$ °C).

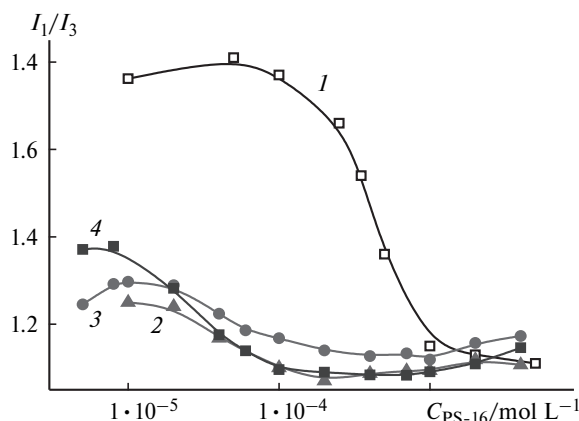


Fig. 4. Ratio of the intensities of the first (373 nm) and third (384 nm) peaks in the fluorescence spectrum of pyrene vs surfactant concentration in an individual solution of PS-16 (1) and in a PAA–PS-16 binary system at the polyelectrolyte concentration 1 (2), 3 (3), and 5 mmol L⁻¹ (4) (pH 4, $t = 25$ °C).

metry (see Table 1). It should be mentioned that the runs of the dependences of the individual and binary systems differ strongly. The polarity parameter (I_1/I_3) decreases noticeably on going from the individual to binary PAA–PS-16 systems (from 1.75 to 1.4). This indicates that the polyelectrolyte chain induces the formation of more densely packed micellar aggregates due to a decrease in the electrostatic repulsion of the head groups of the amphiphile. However, the dependence passes through a minimum, and the polarity parameter begins to increase when reaching the CMC, which is probably related to the formation of individual surfactant micelles.

The results of investigation of the solubilization of the OOT dye in the PAA–PS-16 binary systems are presented in Fig. 5. Two breaks are observed in the concentration

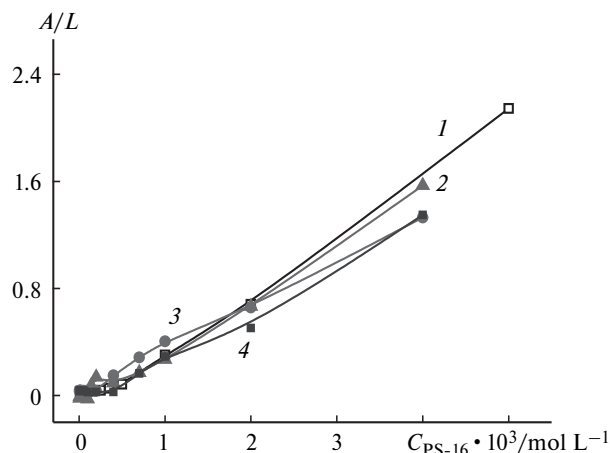


Fig. 5. Absorbance (A) of an individual solution of PS-16 (1) and PAA–PS-16 mixed solutions containing OOT vs surfactant concentration at the PAA concentrations 1 (2), 3 (3), and 5 mmol L⁻¹ (4) (L is the cell thickness (cm), pH 4, $t = 25$ °C; $\lambda = 495$ nm).

curve of the absorbance of OOT at the minimum PAA concentration. The obtained CAC values strongly exceed the tensiometry data (see Table 1). Similar divergences of two methods are probably associated with the fact that spectrophotometry reflects an increase in the solubility (solubilization and retention of the dye) only in aggregates with a high number of molecules. At higher PAA concentrations (3 and 5 mmol L⁻¹), only one inflection remains in the dependence. This inflection insignificantly differs from or coincides with the CMC of an individual solution of PS-16. Probably, at a low concentration of polyelectrolytes their effect, similarly to the effect of low-molecular-weight salt, results in charge neutralization and a denser packing of the aggregates, which favors the retention of dye molecules. Possibly, at high PAA concentrations the aggregation numbers of the PAA–PS-16 mixed system are so low that the aggregates cannot retain dye molecules and, hence, the first break cannot be detected. This explanation agrees well with the values of solubilization capacity (S) and aggregation number (N) of the mixed systems (Table 3). For a small PAA additive to a solution of PS-16, S increases by three times, whereas N decreases by three times. At high PAA concentrations S remains the same as that of an individual solution of PS-16, and the aggregation numbers N decrease insignificantly. This

Table 3. Solubilization capacity (S) and aggregation numbers (N) of PAA–PS-16 mixed systems (pH 4, $t = 25\text{ }^{\circ}\text{C}$)

$C_{\text{PAA}}/\text{mmol L}^{-1}$	$S/(\text{mol OOT}) (\text{mol Surf})^{-1}$	N
0	0.021	42
1	0.059/0.023	14/30
3	0.024	28
5	0.024	37

indicates that, in the latter case, micelles of PS-16 predominantly participate in the solubilization of the dye rather than the PAA–PS-16 mixed system.

The sizes of aggregates in the PAA–PS-16 mixed systems at various PAA concentrations obtained by dynamic light scattering are presented in Fig. 6. The hydrodynamic diameter of individual aggregates of PS-16 is $\geq 5\text{ nm}$ in the whole concentration range. This is a classic size corresponding to spherical micelles. The addition of even low PAA concentration to a solution of PS induces the growth of the aggregates to 94 nm depending on the surfactant concentration. This is probably related to the fact that PAA macromolecule decreases the electrostatic repulsion between surfactant micelles resulting in their approaching and, correspondingly, enlargement of the combined

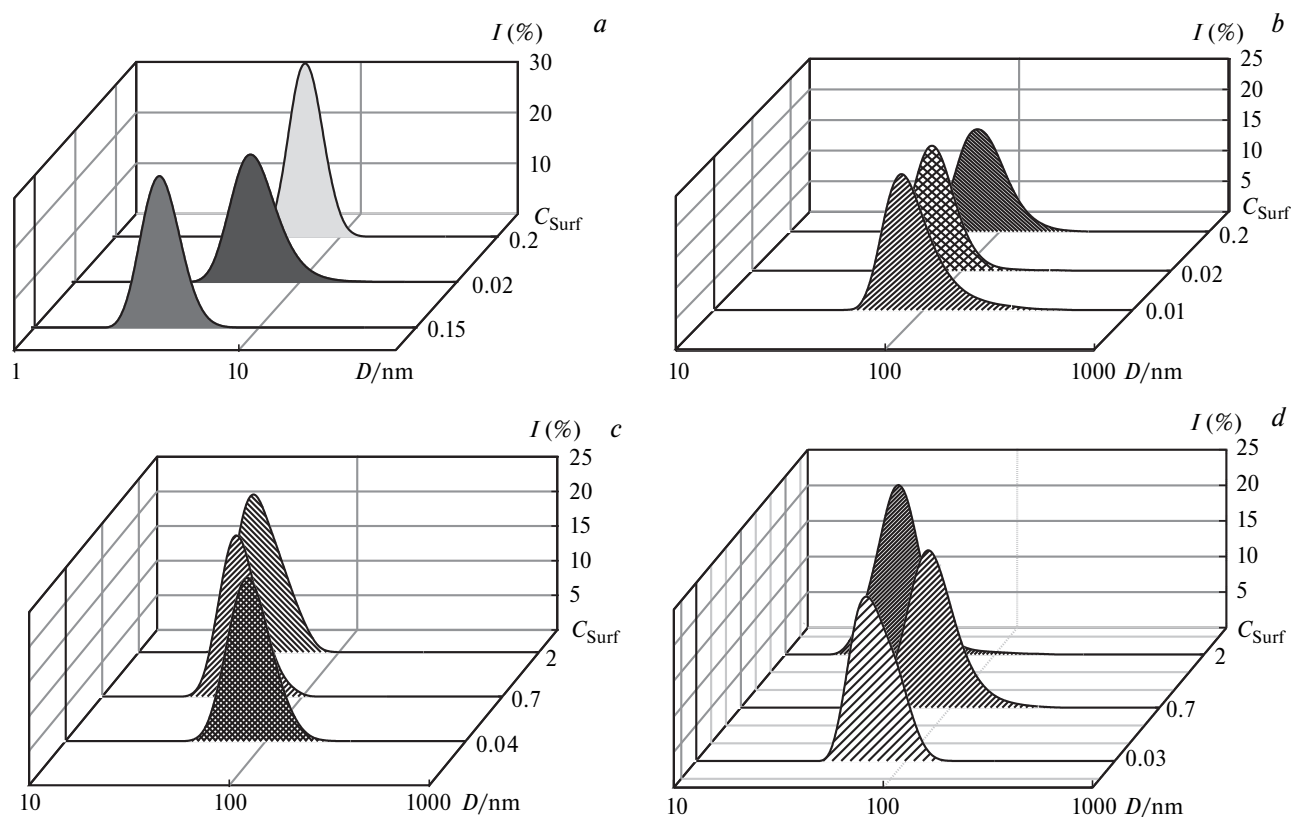


Fig. 6. Hydrodynamic diameter of aggregates vs surfactant concentration ($C_{\text{Surf}}/\text{mmol L}^{-1}$) in an individual solution of PS-16 (a) and in a PAA–PS-16 binary system at the PAA concentrations 1 (b), 3 (c), and 5 mmol L⁻¹ (d) (pH 4, $t = 25\text{ }^{\circ}\text{C}$).

Table 4. Hydrodynamic diameter (D), ζ -potential (ζ), and polydispersity index (PDI) for PAA–PS-16 mixed systems (pH 4, $t = 25\text{ }^\circ\text{C}$)

C_{PAA}	C_{S}	D/nm	ζ/mV	PDI
mmol L ⁻¹				
1	0.01	76.76	-29.6	0.335
	0.02	77.47	-26.2	0.248
	0.2	93.82	27.6	0.179
3	0.04	75.3	-18.4	0.246
	0.7	55.2	48.6	0.156
5	2	35.64	56	0.368
	0.03	70.58	-21.6	0.270
	0.7	90.29	39.6	0.222
	2	34.99	64.5	0.240

aggregates. It is assumed that the components form a classic combined aggregate as a pearl necklace.²¹ The hydrodynamic diameter of the Surf–PE mixed aggregates in the CAC range is 71–77 nm depending on the PAA concentration. At the surfactant concentrations exceeding the CAC values the particle size decreases to 35 nm. This phenomenon is observed only at PAA concentrations of 3 and 5 mmol L⁻¹. It should be mentioned that the hydrodynamic diameter of individual PAA macromolecules is ~250 nm. A decrease in the sizes of Surf–PE aggregates indicates that the surfactants induce compacting of the polyelectrolyte chain by gradually compensating its charge similarly to Surf–DNA systems. The compensation change in the ζ -potential of the mixed system confirms the complex formation of the components *via* the electrostatic mechanism (Table 4).

To conclude, the aggregation and solubilization characteristics of binary systems based on the new pyrrolidinium surfactant with the hexadecyl hydrocarbon radical and hydroxyethyl fragment at the nitrogen atom in the presence of PAA were studied by tensiometry, conductometry, dynamic light scattering, fluorescence spectroscopy, and spectrophotometry. The formation of Surf–PE complexes results in a decrease in the concentration thresholds for nanosized aggregate formation by approximately an order of magnitude. The solubilization capacity of the formed mixed aggregates was tested using the OOT hydrophobic dye. The presence of PAA exerts almost no effect on the solubilization capacity.

This work was financially supported by the Russian Foundation for Basic Research (Project No. 18-43-160015) and the Government of Tatarstan Republic.

References

1. S. Svenson, *Curr. Opin. Colloid Interface Sci.*, 2004, **9**, 201; DOI: 10.1016/j.cocis.2004.06.008.
2. M. C Jennings, K. P. C. Minbiole, W. M. Wuest, *ACS Infect. Dis.*, 2016, **1**, No. 7, 288; DOI: 10.1021/acsinfecdis.5b00047.
3. N. J. Turro, M. Gratzel, A. M. Braun, *Angew Chem. Int. Ed. Engl.*, 1980, **19**, 675; DOI: org/10.1002/anie.198006751.
4. L. Ya. Zakharova, E. P. Zhiltsova, A. B. Mirgorodskaya, A. I. Konovalov, *From Molecules to Functional Architecture. Supramolecular Interactions*, Donetsk, East Publisher House, 2012, 415 pp.
5. K. S. Egorova, V. P. Ananikov, *J. Mol. Liq.*, 2018, **272**, 271; DOI: 10.1016/j.molliq.2018.09.025.
6. M. W. Zhao, L. Q. Zheng, *Chem. Phys.*, 2011, **13**, 1332; DOI: 10.1039/C0CP00342E.
7. G. A. Baker, S. Pandey, S. Pandey, *Analyst*, 2004, **129**, 890; DOI: 10.1039/B410301G.
8. V. P. Schnee, G. A. Baker, E. Rauk, C. P. Palmer, *Electrophoresis*, 2006, **27**, 4141.
9. K. K. Karukstis, J. R. McDonough, *Langmuir*, 2005, **21**, 5716.
10. N. V. Sastry, N. M. Vaghela, V. K. Aswal, *Fluid Phase Equilib.*, 2012, **327**, 22; DOI: 10.1016/j.fluid.2012.04.013.
11. L. Shi, M. Zhao, L. Zheng, *Colloids Surf. A*, 2011, **392**, 305; DOI: 10.1016/j.colsurfa.2011.09.064.
12. L. Zhou, T. Tian, J. Xiao, T. Wang, L. Yu, *J. Mol. Liq.*, 2017, **225**, 50; DOI: 10.1016/j.molliq.2016.10.142.
13. Y. Tian, R. Wei, B. Cai, J. Dong, B. Deng, Y. Xiao, *J. Chromatogr. A*, 2016, **1475**, 95; DOI: 10.1016/j.chroma.2016.11.001.
14. A. B. Mirgorodskaya, E. I. Yackevich, S. S. Lukashenko, L. Ya. Zakharova, A. I. Konovalov, *J. Mol. Liq.*, 2012, **169**, 106; DOI: 10.1016/j.molliq.2012.02.012.
15. L. Ya. Zakharova, A. B. Mirgorodskaya, E. I. Yackevich, V. V. Syakaev, Sh. K. Latypov, A. I. Konovalov, *J. Chem. Eng. Data*, 2012, **57**, 3153; DOI: 10.1021/je300753d.
16. E. A. Vasilieva, S. S. Lukashenko, A. D. Voloshina, A. S. Strobyskina, L. A. Vasileva, L. Ya. Zakharova, *Russ. Chem. Bull.*, 2018, **67**, 1280.
17. D. A. Samarkina, D. R. Gabdrakhmanov, S. S. Lukashenko, A. R. Khamatgalimov, V. I. Kovalenko, L. Ya. Zakharova, *Colloids Surf., A*, 2017, **529**, 990; DOI: 10.1016/j.colsurfa.2017.07.018.
18. A. B. Mirgorodskaya, E. I. Yackevich, D. R. Gabdrakhmanov, S. S. Lukashenko, Yu. F. Zuev, L. Ya. Zakharova, *J. Mol. Liq.*, 2016, **220**, 992; DOI: 10.1016/j.molliq.2016.05.010.
19. M. Zhao, J. Yuan, L. Zheng, *Colloids and Surfaces A: Physicochem. Eng. Aspects*, 2012, **407**, 116.
20. P. Singla, O. Singh, Sh. Chhaba, R. K. Mahajan, *J. Mol. Liq.*, 2018, **249**, 294.
21. K. Holmberg, B. Jönsson, B. Kronberg, B. Lindman, *Surfactants and Polymers in Aqueous Solution*, John Wiley & Sons Ltd., Chichester, 2003, 547 pp.

Received November 30, 2018;
accepted January 10, 2019